# NFKB1/NR3C1-MAPK4 axis regulates the pathology of acute lung injury

**Ling Mao**
Zunyi Medical University
**Ya Zhou**
Zunyi Medical University
**Lin Hu**
Zunyi Medical University
**Shiming Liu**
Zunyi Medical University
**Juanjuan Zhao**
Zunyi Medical University
**Mengmeng Guo**
Zunyi Medical University
**Chao Chen**
Zunyi Medical University
**Zhixu He** ( 854760136@qq.com )
Affiliated Hospital of Zunyi Medical University
**Lin Xu** ( xulinzhouya@163.com )
Zunyi Medical University

**Research**

**Keywords:** MAPK4, ALI, NFKB1, NR3C1, shRNA

**Posted Date:** January 6th, 2020

**DOI:** https://doi.org/10.21203/rs.2.20071/v1

# Abstract

## Background

Acute lung injury (ALI) is a serious disease with highly morbidity and mortality that causes serious health problems worldwide. MAPK4, a member of atypical MAPK family, has been implicated in the development of cancer. Herein, the current study aimed to investigate the possible role of MAPK4 in the pathology of ALI to identify potential candidates for ALI therapy.

## Methods

Murine ALI model was established in WT or MAPK4$^{-/-}$ mice and the expressions of MAPK4 were measured. The survival ratio of ALI model mice was observed. Moreover, the changes of pathologic injury and infiltration of inflammatory cells, as well as the related signaling pathways, in lung tissues were analyzed. Furthermore, the possible molecular mechanism of MAPK4 expression in ALI was analyzed by massARRAY and EMSA assay. Finally, the effect of MAPK4 silencing using shRNA interference on the pathology of ALI was identified.

## Results

Data showed that MAPK4 was up-regulated in lung tissues in LPS-induced murine ALI model. Importantly, MAPK4 deficiency mice exhibited prolonged survival time after LPS challenge, accompanied by alleviated inflammatory injury in lung tissues characterized with reduced production of pro-inflammatory cytokines, infiltration of immune cells and altered transduction of related signaling pathways. Besides, massARRAY results showed no aberrant change in CpG methylation levels between control and ALI mice. Bioinformatics analysis and EMSA assay showed that transcriptional factor NFKB1 and NR3C1 could negatively regulate the expression of MAKP4. Finally, MAPK4-shRNA treatment could ameliorate the pathology of lung tissues and prolong the survival time of mice after LPS challenge.

## Conclusions

Our data demonstrated that MAPK4, orchestrated by NFKB1 and NR3C1, could regulate the pathology of ALI, indicating that MAPK4 might be a new therapeutic target for ALI treatment.

# Background

Acute lung injury (ALI) and it's more serious form acute respiratory disease syndrome (ARDS) are critical diseases characterized with diffuse inflammations in lungs, which could be triggered by various pathologies, such as sepsis and severe trauma [1, 2]. Despite numerous therapeutic strategies have been used to ALI treatment [3-5], the worldwide incidence and mortality of ALI are still showing no sign of amelioration in the past decades [6, 7]. One of the reasons why these therapeutic strategies are invalid is that the molecule mechanism of development of ALI is very complex and remains to be fully elucidated. Therefore, further investigation on the molecular mechanism of pathology of ALI is still urgent and critical

for the development of novel therapeutic strategies against ALI, which ultimately benefits the clinical outcome of ALI patients.

MAPK4 (alias ERK4, p63 MAPK) is the member of atypical MAPKs and closely related to MAPK6 with 73% amino acid identity in the kinase domain [8]. Accumulating evidences have shown that MAPK4 is implicated in the development of various diseases including cancer and infection diseases [9-11]. To lung development and diseases, *Rousseau et al.* found that the loss of MAPK4 didn't affect intrauterine growth and lung maturation [12], suggesting that MAPK4 might be not involved in the development of lung. Interestingly, *El-Aarag et al.* found that MAPK4 was closely related to the development of lung cancer [13]. Most recently, *Wang et al.* further reported that MAPK4 overexpression could promote the progression of lung cancer, indicating MAPK4 is a potential target for lung cancer therapy [14]. These researches have raised an interesting question that MAPK4 might be, as an important regulator, involved in the development of lung diseases. However, up to now, the potential role of MAPK4 in the lung related inflammatory diseases including ALI remains largely unknown.

To this aim, in present study, we evaluated the expression of MAPK4 in LPS-induced murine ALI and accessed the possible effects of MAPK4 deficiency on the pathology of ALI. We found that MAPK4 was up-regulated in lung tissues of LPS-induced murine ALI model. Importantly, MAPK4 deficiency could attenuate the inflammatory injury of ALI, accompanied by reduced infiltration of immune cells and production of pro-inflammatory cytokines, as well as altered transduction of related signaling pathways. Moreover, we found that transcription factor NFKB1 and NR3C1 could negatively regulate the expression of MAPK4 by binding to the core sequence of MAPK4 promoter. Importantly, MAPK4-shRNA treatment could significantly reduce the pathology of lung tissues and prolong survival time of ALI mice. Altogether, our study reveals an unknown role of MAPK4 in the pathology of ALI, indicating that MAPK4 might be a new therapeutic target for clinic therapy against ALI.

# Materials And Methods

### Mice

MAPK4 deficiency ($MAPK4^{-/-}$) mice breeding pair in a C57BL/6 background were purchased from The Jackson Laboratory (027666). Animals were housed under specific pathogen-free conditions at Zunyi Medical University.

### Cell culture

Raw264.7 cells were purchased from Conservation Genetics CAS Kunming Cell Bank (KCB200603YJ), and were cultured in high glucose DEME containing 10% fetal bovine serum at 37°C in 5% $CO_2$.

### Establishment of ALI Model

WT and MAPK4$^{-/-}$ mice (7 to 9 week-old) were challenged with i.p. injection of 10mg/kg LPS (Escherichia coli 0111:B4; Sigma) dissolved in sterile PBS as shown in our previous study [17]. Then the body weight and lung weight index (lung weight/body weight) was detected at indicated time.

### Bronchoalveolar Lavage

Immediately after euthanasia, 1 ml aliquots of PBS were slowly infused in the murine lungs through the tracheostomy and then withdrawn gently. This lavage was repeated three times using the same syringe. The collected lavage fluid was stored in a 10ml tube on ice. The fluid was centrifuged at 1000rpm and 4°C for 10 min, and the cell sediment was washed with PBS. The cell-free supernatant was centrifuged again at 14,000g and 4°C for 10 min, stored at −80°C and used for determination of cytokines content via ELISA. To the pellet, red blood lysis buffer (Solarbio, R1010) were used for 15 min and washed with PBS. Next, the pellet was resuspended for analysis.

### Lung edema determination

Lungs from mice were excised and completely dried in the oven at 60°C 24h for calculation of lung wet/dry ratio.

### Histology and immunohistochemistry

Lung tissues were fixed in 4% paraformaldehyde, embedded in paraffin, and cut into 4μm-thick sections. For histology analysis, the lung sections were stained with hematoxylin and eosin (HE). For immunohistochemistry, the lung sections were deparaffinized with xylene and rehydrated in graded ethanol (100% to 70%). To eliminate endogenous peroxidase activity, the slides were treated with 3% $H_2O_2$ for 30min and washed with PBS. Then, the slides were blocked with Goat serum (BOSTER, AR1009 ) for 2h at room temperature and incubated overnight at 4°C with corresponding antibodies (p-JNK: Cell Signaling Technology, 4668; p-p38 MAPK: Cell Signaling Technology, 42390). After washed with PBS, the slides were incubated with secondary antibodies and visualized with DAB kit (Solarbio, DA1010). Finally, the slides were counterstained with hematoxylin and analyzed by Olympus microscope.

### Immunofluorescence

Lung tissues were fixed in 4% paraformaldehyde, embedded in paraffin, and cut into 4μm-thick sections. Briefly, the slides were incubated with corresponding primary antibodies (MAPK4: Proteintech, 26102-1-AP; F4/80: abcam, ab60343 ) and secondary antibody (Alexa 647: Cell Signaling Technology, 4414S) after deparaffinization and rehydration. Then, the slides were counterstained with DAPI (Beyotime, C1002) and observed by Olympus microscope.

### RNA extraction and quantitative real time PCR

Total RNA was isolated from mice lungs using RNAiso Plus (TAKARA, 9108) according to manufacture's instructions. RNA was quantified and reverse-transcribed according to manufacture's instructions

(TAKARA, RR037A). SYBR Green-based real time quantitative PCR reactions (TAKARA, RR820A) and gene specific primers were used. The following primers were used: IL-1β forward: 5'-TGCCACCTTTTGACAGTGATG-3', reverse: 5'-AAGGTCCACGGGA

AAGACAC-3'; IL-6 forward: 5'-GGAAATCGTGGAAATGAG-3', reverse: 5'-AGGACTCTGG

CTTTGTCT-3'; TNF-α forward: 5'-CAGGGGCCACCACGCTCTTC-3', reverse: 5'-TTTGTGA

GTGTGAGGGTCTGG-3'; IL-4 forward: 5'-AACGAGGTCACAGGAGAA-3', reverse: 5'-CCT

TGGAAGCCCTACAGA-3'; IL-10 forward: 5'-TACAGCCGGGAAGACAATAA-3', reverse: 5'-

AGGAGTCGGTTAGCAGTATG-3'; TGF-β forward: 5'-GGCGGTGCTCGCTTTGTA-3', revers-

e: 5'-TCCCGAATGTCTGACGTATTGA-3'; GAPDH forward: 5'-TCCATGACAACTTTGGCAT

TG-3', reverse: 5'-TCACGCCACAGCTTTCCA-3'. Gene expression levels were quantified using Bio-Rad CFX96 detection system (Bio-Rad Laboratories). With GAPDH was used as internal reference, the expressions of genes were calculated by using the comparative threshold cycle (Ct) method.

## DNA extraction and methylation analysis

Genomic DNA was extracted from 12 lungs of control and ALI model mice by using DNeasy Blood and Tissue kit (QIAGEN, 69504) according to manufacture's instructions. The quality and quantified were evaluated by gel electrophoresis and a NanoDrop spectrophotometer (Thermo). The genomic DNA from each sample was treated with sodium bisulfite using an EZ DNA methylation kit (Zymo Reasearch). The MassARRAY platform (The Beijing Genomics Institute) was used for quantitative analysis of MAPK4 methylation. We used the primers (5'-aggaagagagGGGTGGGTTTTATTAGAGATAGTGG-3', 5'-cagtaatacgactcactatagggagaaggct

AATCTAAATCCCAACTAAATAATCCC-3') to amplify the region of each promoter. Altogether, 35 CpG sites were tested in this region. The spectra methylation ratios of each CpG site were generated by MassARRAY EpiTYPER software (Agena).

## FCM

Surface markers of series immune cells were detected by flow cytometry (FCM) with Beckman Gallios (Beckman Coulter, Inc.). FCM was performed on Beckman Gallios with CellQuest Pro software using directly anti-Mouse monoclonal conjugated antibodies against the following markers: F4/80-Percp-Cy5.5 (clone: BM8; no.45-4801-82), F4/80-FITC (clone:BM8; no.11-4801-85), γδT-APC (clone: eBioGL3; no.17-5711-81), NK1.1-APC (clone: PK136; no.17-5941-81), CD11c-PE (clone: N418; no.12-0114-82), CD4-FITC (clone: GK1.5; no.11-0041-86), CD8-Percp-Cy5.5 (clone: 53-6.7; no.45-0081-82), CD62L-PE (clone: MEL-14; no.12-0621-81), CD69-APC (clone:H1.2F3; no.17-0691-82), Gr-1-FITC (clone:RB6-8C5; no.11-5931-81), CD86-APC (clone: GL1; no.17-0682-81), MHCII-PE (clone: M5/114.15.2; no.12-5321-81), with

corresponding isotype-matched (eBioscience). Cells were stained with corresponding antibodies (1:100) at 4°C for 30min, respectively. After washing twice, stained cells were analyzed with a Beckman coulter flow cytometer.

## ELISA

The protein levels of IL-1β, TNF-α, IL-6, IL-4 and TGF-β in BAL fluid were detected by ELISA according to manufacture's instructions, respectively (eBioscience).

## Western blot

Lung tissues were homogenized in ice-clod lysis buffer (KeyGEN BioTECH, KGP2100) according to manufacture's instructions. Equal amounts of protein were separated by 10% SDS-PAGE and protein were transferred onto polyvinyldifluoride membranes. Membranes were incubated with 5% skim milk in PBS for 1 hour. Immunobloting was performed using mAbs to MAPK4 (Abacam, ab96816), AKT (Cell Signaling Technology, 4691), p-AKT (Cell Signaling Technology, 4060), ERK1/2 (Cell Signaling Technology, 4695), p-ERK1/2 (Cell Signaling Technology, 4370), p-NF-κB (Cell Signaling Technology, 3039S), p-JNK (Cell Signaling Technology, 4668), p-p38 MAPK (Cell Signaling Technology, 42390), MK5 (Cell Signaling Technology, 7419S), p-MK5 (Biobyt, A5005) and GAPDH (Cell Signaling Technology, 5174). Membranes were washed in PBST and subsequently incubated with a secondary anti-rabbit antibody conjugated to HRP (Cell Signaling Technology, 7074S). The signal was detected and analyzed using Bio-Rad ChemiDoc MP Imaging System (Bio-Rad Laboratories). GAPDH was used as internal reference.

## Plasmid construction

Series versions of truncated MAPK4 promoter (NCBI, NC_000084.6 74064925 to 74067228) were synthesized and cloned into pGL3.0 basic vector between KpnI and MluI sites (Gene Create, GS1-1905109). And we synthesized MAPK4-shRNA (forward: 5'-GATCCGCAAGGGTTATCTG

TCAGAAGGGTTGTTCAAGAGACAACCCTTCTGACAGATAACCCTTGTTTTTTACGCGTG-3', reverse: 5'-AATTCACGCGTAAAAAACAAGGGTTATCTGTCAGAAGGGTTGTCTCT

TGAACAACCCTTCTGACAGATAACCCTTGCG-3') and control group (forward:5'-GATCCG

CAAATTGGTCTGACTGGAAGGGTTGTTCAAGAGACAACCCTTCCAGTCAGACCAATTTGTTTTTTACGCGTG-3', reverse: 5'-AATTCACGCGTAAAAAACAAATTGGTCTGACTGGA

AGGGTTGTCTCTTGAACAACCCTTCCAGTCAGACCAATTTGCG-3'), then cloned into pLVX-shRNA1 vector between BamHI and EcoRI sites. These vectors were extracted by using EndoFree Plasmid Maxi Kit (12123). After verified by DNA sequencing, these vectors were used for further study.

## Transfection and luciferase reporter assay

Raw264.7 cells were transfected with series of truncated MAPK4 promoter vectors by using Lipofectamine 3000 reagent (Invitrogen, L3000015) according to manufacture's instruction. After 24 hours, the cells were detected for Luciferase activity according to manufacture's instruction (Promega).

### EMSA

Nuclear proteins were extracted from the lung tissues of control or ALI mice by using Nuclear and Cytoplasmic Extraction Regents (Thermo Fisher, 78833) according to manufacture's instruction. The biotinated and un-biotinated probes (NFKB1: forward:5'- gagctccacatcgcgacatcc

cttcctcaaggac-3', reverse: 5'- CTCGAGGTGTAGCGCTGTAGGGAAGGAGTTCCTG-

3'; NR3C1: forward:5'-gttgctggggctccagctgtccccgccgcagca-3', reverse: 5'-CAACGACCCCGAGGTCGACAGGGGCGGCGTCGT-3') were synthesized (Sangon). The electrophoretic mobility shift assays for each transcription factor were performed using Chemiluminescent Nucleic Acid Detection Module Kit (Thermo Fisher, 89880) according to manufacture's instruction.

### Statistical analysis

Statistical analysis was performed using GraphPad Prism 5 software. 1-way ANOVA followed by Bonferroni's post-hoc was applied for multiple comparisons and student's t-test was used when two conditions were compared. $P$ <0.05 was considered statistically significant and two-sided tests were performed. All date are shown as a mean ± standard error of the mean (SEM). Survival was evaluated by the Kaplan-Meier method.

## Results

### MAPK4 is up-regulated in the lung tissues of murine ALI model.

To investigate the possible role of MAPK4 in the development of ALI, we first detected the expression of MAPK4 in LPS-induced ALI model (Figure 1A). As shown in figure 1B, the relative expression of MAPK4 increased obviously in the lung tissues and reached the peak at 24 hours post LPS challenge ($P$<0.05). Moreover, compared with that in control group, the expression level of MAPK4 protein in lung tissues in ALI group also increased significantly (Figure 1C, $P$<0.05). To confirm this phenomenon, we also verified the expression of MAPK4 in lung tissues using immunohistochemistry assay and obtained similar results (Figure 1D).

Microphages played important roles in the inflammatory process of ALI [15, 16]. Then, we also detected the infiltration of $F4/80^+$ cells in lung tissues in LPS-induced ALI model. Immunofluorescence assay data showed that the infiltration of $F4/80^+$ cells increased obviously in the lung tissues in ALI model (Figure 1E), which was consistent with our previous work [17]. Moreover, in line with above findings, the expression of MAKP4 protein was also elevated in the lung tissues (Figure 1E). Interestingly, we found

that there was co-localization of F4/80$^{+}$ cells and MAPK4 protein in lung tissues (Figure 1E). Altogether, these findings indicated that MAPK4 might be involved in the pathology of ALI.

### MAPK4 deficiency ameliorates the pathology of ALI.

Next, we observed the possible effects of MAPK4 deficiency on the pathology of ALI. As shown in figure 2A, MAPK4$^{-/-}$ mice had a prolonged survival time compared with that in LPS-treated WT mice ($P$<0.05). Even though the body weight index and lung weight index did not change significantly (Figure 2B and 2C, $P$>0.05), the lung edema reduced obviously in LPS-treated MAPK4$^{-/-}$ mice compared with that in LPS-treated WT mice (Figure 2D, $P$<0.05), which was a typical symptom of inflammation in lung injury [18]. Moreover, the protein level of BAL fluid also decreased markedly in LPS-treated MAPK4$^{-/-}$ mice (Figure 2E, $P$<0.05). Furthermore, HE staining results showed that the infiltration of inflammatory cells and alveolar interstitium thickening in lungs significantly reduced in LPS-treated MAPK4$^{-/-}$ mice (Figure 2F). Hence, these data demonstrated that MAPK4 deficiency could obviously reduce the pathology of LPS-induced ALI.

### Loss of MAPK4 alters the production of related cytokines in ALI.

Previous evidences have shown that pro-inflammatory cytokines, such as IL-1β and TNF-α, were involved in the pathology of lung injury [19, 20]. To confirm the effects of MAPK4 deficiency on the pathology of ALI, we further detected the levels of inflammatory related cytokines in ALI mice. As shown in figure 3A-F, the mRNA levels of IL-1β and TNF-α in lung tissues in LPS-treated MAPK4$^{-/-}$ mice significantly decreased compared with those in LPS-treated WT mice ($P$<0.05). By contrast, the mRNA levels of anti-inflammatory cytokines TGF-β, IL-4 and IL-10 were markedly higher in LPS-treated MAPK4$^{-/-}$ mice ($P$<0.05). To verify these data, we also analyzed the protein levels of these cytokines in BAL fluid from LPS-treated WT or MAPK4$^{-/-}$ mice and obtained similar results (Figure 3G-K, $P$<0.05). Thus, these results demonstrated that MAPK4 deficiency could affect the production of related inflammatory cytokines in ALI.

### Loss of MAPK4 affects the immune cells composition in BAL fluid of ALI.

The infiltration and activation of related immune cells in lung tissues were involved in inflammatory response in ALI [21], therefore we assessed the composition of related immune cells in BAL fluid from LPS-treated WT or MAPK4$^{-/-}$ mice. As shown in figure 4A, compared with that in LPS-treated WT mice, the total numbers of infiltrated cells in BAL fluid significantly decreased in LPS-treated MAPK4$^{-/-}$ mice ($P$<0.05). Next, we further measured the changes on proportion of innate immune cells, including Gr-1$^{+}$ neutrophils, F4/80$^{+}$ macrophages, γδT$^{+}$ cells, NK1.1$^{+}$ cells and CD11c$^{+}$ dendritic cells (DCs) in BAL fluid from LPS-treated WT or MAPK4$^{-/-}$ mice. Data showed that the proportions and cell counts of Gr-1$^{+}$ neutrophils, γδT cells and CD11c$^{+}$ DCs obviously decreased in LPS-treated MAPK4$^{-/-}$ mice (Figure 4B, 4C and 4E, $P$<0.05). Although the proportions of F4/80$^{+}$ macrophages and NK1.1$^{+}$ cells did not change significantly, the cell counts of these cells obviously reduced in BAL fluid from LPS-treated MAPK4$^{-/-}$ mice (Figure 4C and 4E, $P$<0.05). We further analyzed the expression of membrane molecule MHC II and CD86,

which are important functional molecules on F4/80$^+$ macrophages [22]. Data showed that the proportion of MHC II$^+$ on macrophages significantly increased in LPS-treated MAPK4$^{-/-}$ mice (Figure 4D, $P$<0.05), indicating MAPK4 deficiency might affect the function of macrophages.

Moreover, we also investigated the change on adaptive immune cells in BAL fluid from LPS-treated WT or MAPK4$^{-/-}$ mice. Date showed that the proportion and cell count of CD4$^+$ T cells significantly decreased in LPS-treated MAPK4$^{-/-}$ mice (Figure 4F, $P$<0.05); even though the proportion of CD8$^+$ T cells increased, the cell count of CD8$^+$ T cells did not change significantly (Figure 4F, $P$>0.05). Meanwhile, we further detected the expression of CD62L and CD69 on both CD4$^+$ T cells and CD8$^+$ T cells, respectively. Results showed that the proportions and cell counts of CD62L$^+$ and CD69$^+$ on CD4$^+$ T cells obviously decreased in LPS-treated MAPK4$^{-/-}$ mice (Figure 4G, $P$<0.05), indicating the reduced activation of CD4$^+$ T cells in LPS-treated MAPK4$^{-/-}$ mice. However, the cell counts of CD62L$^+$ and CD69$^+$ on CD8$^+$ T cells did not change significantly (Figure 4H, $P$>0.05). Finally, to verify these phenomenons, we further analyzed the proportions and cell counts of related immune cells in spleen of WT or MAPK4$^{-/-}$ mice after LPS treatment and obtained similar results (Additional file 1). Collectively, these results demonstrated that MAPK4 deficiency could affect the compositions and functions of infiltrated immune cells in ALI, which could contribute to the attenuated pathology of ALI.

### MAPK4 deficiency alters the transduction of related signaling pathways in ALI.

It is well known that AKT, ERK1/2, JNK, p38 MAPK and NF-κb signaling pathways play important roles in the development of inflammation response [23-25]. To elucidate whether MAPK4 deficiency ameliorated the pathology of ALI was related to these signaling pathways, we detected the transduction of those signaling pathways in lung tissues from LPS-treated WT or MAPK$^{-/-}$ mice, respectively. Western blot results showed that the expression levels of p-AKT, p-JNK and p-p38 MAPK significantly decreased in LPS-treated MAPK4$^{-/-}$ mice compared with these in LPS-treated WT mice (Figure 5A, $P$<0.05). Previous study has shown that MK5 was a downstream molecular of MAPK4 [26], and we also found that the expression level of p-MK5 markedly reduced in LPS-treated MAPK4$^{-/-}$ mice (Figure 5B, $P$<0.05). To confirm these data, we further analyzed the expressions of p-p38 MAPK and p-MK5 in lung tissues by immunohistochemistry assay and similar results were obtained (Figure 5C). Token together, these data indicated that the protective effects of MAPK4 deficiency on the pathology of ALI was related to the altered transduction of AKT, JNK, p38 MAPK and MK5 signaling pathways.

### NFKB1 and NR3C1 negatively regulate the expression of MAPK4 in ALI.

Next, we further explore the potential molecular mechanism of up-regulated expression of MAPK4 in ALI. Recent decades, DNA methylation is commonly invoked as a mechanism for transcriptional repression [27-29], we wondered whether DNA demethylation of CpG island in MAPK4 promoter enhanced the expression of MAPK4 in LPS-induced ALI. Expectedly, bioinformatics analysis indicated that there was a CpG island in the promoter of MAPK4 (Figure 6A). However, sequenom massARRAY assay data showed

that the CpG methylation level of MAPK4 promoter did not change significantly between control and ALI mice (Figure 6B and 6C, $P>0.05$), indicating that DNA demethylation maybe not contribute to the up-regulation of MAPK4 in ALI.

To further analyze the molecular mechanism of up-regulated MAPK4 in ALI, we next sought to screen the core transcription factors of MAPK4 promoter and performed 3' deletion assay to access the core sequence of MAPK4 promoter (Figure 7A). Results showed that luciferase activity increased significantly between 2.2kb and 1.5kb region in MAPK4 promoter, indicating that this region might be the core sequence of MAPK4 promoter. Then, we utilized transcription factor binding sites (TFBS) prediction databases (TRANSFAC and JASPAP) to analyze the potential transcription factors and found 8 candidate transcription factors, including Sp1 (trans-acting transcription factor 1), MyoD (myogenic differentiation), Egr-1 (early growth response 1), NFKB1 (nuclear factor kappa B subunit 1), ETF (TEA domain family member 2), PU.1 (spleen focus forming virus proviral integration oncogene), NR3C1 (nuclear receptor subfamily 3 group C member 1, encoded glucocorticoid receptor) and MRF4 (myogenic factor 6) (Figure 7C and 7D). Previous studies showed that Sp1, Egr-1, NFKB1, NR3C1 and PU.1 have been reported to play roles in inflammatory response [30-34], so we analyzed the mRNA levels of these transcription factors and found that, compared with those in control group, the mRNA levels of NFKB1, NR3C1 and Egr-1 were obviously lower in ALI group, while the mRNA levels of Sp1 and PU.1 significantly increased (Figure 7E, $P<0.05$). Because the luciferase activity results showed that the putative transcription factors could negatively regulate MAPK4 expression and accumulating evidences have shown that NFKB1 and NR3C1 were anti-inflammatory genes [31, 32], so we presumed that NFKB1 and NR3C1 might be critical transcription factors in regulating MAPK4 expression in ALI. Expectedly, further analysis showed that the protein levels of NFKB1 and NR3C1 decreased obviously in lung tissues in ALI mice (Figure 7F, $P<0.05$), which is consistent with our above data. Importantly, electrophoretic mobility shift assay further showed that NFKB1 and NR3C1 could directly bind to the promoter of MAPK4 (Figure 7G and 7H), Together, these results demonstrated that NFKB1 and NR3C1 are new core transcription factors in regulating the expression of MAPK4 in ALI.

### MAPK4-shRNA treatment protects mice against LPS-induced ALI.

Finally, we further explored whether MAPK4 might be a novel valuable target in ALI treatment using shRNA technique. As shown in figure 8A and B, compared with that in control group, the expression of MAPK4 decreased markedly in MAPK4-shRNA treatment group ($P<0.05$). Expectedly, the edema and inflammatory injury of lung tissues reduced significantly in MAPK4-shRNA treatment group (Figure 8C and 8D). Meanwhile, the levels of pro-inflammatory cytokines, including IL-1β and TNF-α, decreased significantly (Figure 8E, $P<0.05$); conversely, the level of anti-inflammatory cytokine IL-10 increased obviously in MAPK4-shRNA treatment group (Figure 8E, $P<0.05$). To confirm the effect of MAPK4-shRNA in the transduction of related signaling pathways, we further analyzed the expressions of these pathways. Date showed that the expression levels of p-AKT, p-JNK and p-p38 MAPK significantly decreased in MAPK4-shRNA treatment mice compared with these in LPS-treated WT mice (Figure 8F), which were consistent with our above data. Of note, MAKP4-shRNA treatment could prolong survival time

of ALI mice (Figure 8G). All together, these data demonstrated that MAPK4-shRNA treatment could effectively ameliorate the pathology of ALI, indicating it might be a new valuable therapeutic target in ALI treatment.

# Discussion

Mitogen activated protein kinases (MAPKs) are protein Serine/Threonine kinases that comprise conventional MAPKs (ERK1/2, p38, ERK5, JNK) and atypical MAPKs (ERK3/4, ERK7/8, NLK), which could convert extracellular stimuli into a wide range of cellular responses [35,36]. Accumulating evidences have demonstrated that conventional MAPKs were involved in the development of inflammation related lung diseases [37]. For example, *Carnesecchi et al.* found that hyperoxia led to the phosphorylation of JNK and ERK, which was involved in cell death signaling and was related with oxidative stress induced acute lung injury [38]. *Schnyder-Candrian et al.* showed that LPS induced ARDS was mediated by p38 MAPK [39]. However, the studies focused on the roles of atypical MAPKs in inflammation related diseases is still scare. Herein, we found that the expression of MAPK4 was up-regulated in ALI. Importantly, we verified that MAPK4 deficiency could significantly ameliorate the pathology of lung tissues, accompanied with reduced infiltration of immune cells and production of pro-inflammatory cytokines, including IL-1β and TNF-α. Therefore, our current data revealed an unknown role of MAPK4, a member of atypical MAPKs, in the pathology of ALI, which might provide a light on the role of atypical MAPKs in inflammation related diseases. Given the fact that immune cells, such as macrophages, expressed MAPK4 in ALI model, then, which types of immune cells are mainly involved in the pathology process of ALI in the condition of MAPK4 deficiency need to be further elucidated.

It is well known that there are complex networks among AKT, JNK and ERK pathways in biological process. For example, *Wu et al.* reported that IL-22 tethered to apolipoprotein A-I could ameliorate acute liver injury by altering EKT and AKT signaling transductions [40], suggesting the complicated connection among these pathways in liver injury. Moreover, in our previous work, we also found that miR-7 could affect the development of ALI, accompanied with altered transduction of AKT and ERK pathways [17]. In present study, we found that MAPK4 deficiency could decrease the expressions of p-AKT, p-JNK and p-p38 MAPK in ALI model. Similarly, *Wang et al.* demonstrated that MAPK4 directly bound and activated AKT by phosphorylation of the activation loop at threonine 308, thereby inducing oncogenic outcomes, including transforming prostate epithelial cells into anchorage-independent growth [14]. Therefore, these data might highlight the underlying connection among conventional MAPKs, atypical MAPKs and other signaling pathways. Finally, previous work found that MAPK4 could regulate MK5 thereby controlling the biological process [26]. Consistent with this finding, we also noticed that, in present study, the level of p-MK5 significantly decreased in the condition of MAPK4 deficiency. Interestingly, *Perander et al.* reported that the expression of DUSP2 could inhibit ERK3 and ERK4 mediated activation of its downstream substrate MK5 [41]. Therefore, further study on the roles of other couple molecules of MAPK4, which did not be screened in current study, is much valuable for illustration on the exact connections among MAPK4/MK5, AKT and other signaling pathways in the pathology of ALI.

Recent decades, numerous studies have revealed that the mechanisms of transcriptional regulation on gene expression were complex, including DNA methylation and transcriptional factors [42-45]. In present study, bioinformatics analysis showed that there was a CpG island in the promoter of MAPK4. Unexpectedly, we found that there was not significant change in CpG methylation level of MAPK4 promoter in ALI model, indicating that DNA demethylation of MAPK4 promoter might not be critical for the up-regulation of MAPK4 in ALI. Interestingly, we identified the core sequence region of MAPK4 promoter (-470 to +173 relative to the TSS). Of note, we verified that two important transcription factors NFKB1 and NR3C1 could directly bind to the core sequence region of MAPK4 promoter, indicating that NFKB1/NR3C1 negatively regulated the expression of MAPK4 in ALI. Consistent with these findings, *Adamzik et al.* showed that genotypes of NFKB1 promoter polymorphism were associated with the severity in ARDS [46]. Moreover, *Zhao et al.* reported that somatostatin could alleviate the pathology of murine ALI, which was closely related with the affinity of glucocorticoid receptor [47]. Therefore, these data further verified the important role of NFKB1/NR3C1 in the pathology of ALI.

The gene silencing technique, including antisense oligonucleotides (ASOs) and short hairpin RNA (shRNA), could effectively knock down the expressions of interesting genes and was an important strategy for gene therapy against various diseases [48-51]. Our previous studies showed that ASOs against miR-21 might be a useful strategy to alter the expression of miR-21 in colon carcinoma cells and be helpful for the development of miR-21-based therapeutic strategies against clinical colon carcinoma [52]. *Wei et al.* reported that MALAT1-shRNA treatment alleviated the inflammatory injury after lung transplant ischemia-reperfusion by downregulating IL-8 and inhibiting infiltration and activation of neutrophils [53]. Hence, we monitored the possible effects of MAPK4-shRNA treatment on the pathology of ALI. Expectedly, MAPK4 silencing could obviously reduce the pathology of lung tissues in ALI model, accompanied by altered levels of inflammatory cytokines and transduction of related signaling pathways. Importantly, we noticed that MAPK4 silencing could prolong the survival time of ALI mice. Combining these data, we demonstrated that MAPK4 might be a new valuable therapeutic target for ALI therapy.

# Conclusions

For the first time, our study revealed an unknown role of MAPK4, which was regulated by NFKB1 and NR3C1, in the pathology of ALI. Importantly, MAPK4 silencing could obviously reduce the pathology of lung tissue in ALI model. This work might provide a novel insight for future ALI therapy.

# Declarations

### Ethical approval and consent to participate

All animal experiments were performed according to the guidelines for the Care and Use of Laboratory Animals (Ministry of Health, China, 1998). The experimental procedures were approved by the ethical

guidelines of Zunyi Medical University laboratory Animal Care and Use committee (permit number 2013016).

### Consent for publication

All listed authors consent to the submission and all data are used with the consent of the person generating the data.

### Availability of supporting data

The datasets generated and analyzed during the current study are available from the corresponding author on reasonable request.

### Competing interests

The authors declare that they have no conflict of interest.


### Funding

This manuscript was supported by National Natural Science foundation of China (31760258; 81871313;81960509), Program for High level innovative talents in Guizhou Province (QKH-RC-2016-4031), Program for Excellent Young Talents of Zunyi Medical University (15ZY-001), Project of Guizhou Provincial Department of Science and Technology (QKH-JC-2018-1428; QKH-SZ-2019-5406; QKH-LH-2015-7542) and Program for Science and Technology Joint Fund Project in Zunyi Science and Technology Bureau and Zunyi Medical University (ZSKH-SZ-2016-38).


### Author contributions

Ling Mao performed the most experiments, analyzed the data, drafted the manuscript; Ya Zhou analyzed the data, drafted the paper; Lin Hu, Shiming Liu and Juanjuan Zhao performed the FCM and Western blot experiments, Mengmeng Guo analyzed the data, Chao Chen edited the manuscript; Zhixu He conceived and designed the experiments, edited the manuscript; Lin Xu conceived and designed the experiments, analyzed the data, edited the manuscript. All authors read and approved the final manuscript.


### Acknowledgements

Not applicable


## Abbreviations

ALI: acute lung injury; ARDS: acute respiratory distress syndrome; BALF: bronchoalveolar lavage fluid; EMSA: Electrophoretic Mobility Shift Assay; IFN: Interferon; IL: Interleukin; LPS: Lipopolysaccharide; MAPK4: mitogen activated protein kinase 4; NFKB1: nuclear factor kappa B subunit 1; NR3C1: nuclear receptor subfamily 3 group C member 1; shRNA: short hairpin RNA; TNF: Tumor necrosis factor

# References


1. Thompson BT, Chambers RC and Liu KD. Acute respiratory distress syndrome. N Engl J Med. 2017;377(6):562-572.

2. Zhou Y, Li P, Goodwin AJ, Cook JA, Halushka PV, Chang E, et al. Exosomes from endothelial progenitor cells improve outcomes of the lipopolysaccharide-induced acute lung injury. Crit Care. 2019;23(1):44.

3. Vettorazzi S, Bode C, Dejager L, Frappart L, Shelest E, Klaßen C, et al. Glucocorticoids limit acute lung inflammation in concert with inflammatory stimuli by induction of SphK1. Nat Commun. 2015; 6:7796.

4. Bellingan G, Maksimow M, Howell DC, Stotz M, Beale R, Beatty M, et al. The effect of intravenous interferon-beta-1a (FP-1201) on lung CD73 expression and on acute respiratory distress syndrome mortality: an open-label study. Lancet Respir Med. 2014;2(2):98-107.

5. Matthay MA, Goolaerts A, Howard JP and Lee JW. Mesenchymal stem cells for acute lung injury: preclinical evidence. Crit Care Med. 2010;38(10 Suppl):S569-73.

6. Rubenfeld GD, Caldwell E, Peabody E, Weaver J, Martin DP, Neff M, et al. Incidence and outcomes of acute lung injury. N Engl J Med. 2005;353(16):1685-93.

7. Eworuke E, Major JM and Gilbert McClain LI. National incidence rates for Acute Respiratory Distress Syndrome (ARDS) and ARDS cause-specific factors in the United States (2006-2014). J Crit Care. 2018;47:192-197.

8. Coulombe P and Meloche S. Atypical mitogen-activated protein kinases: structure, regulation and functions. Biochim Biophys Acta. 2007;1773(8):1376-87.

9. Song L, Du A, Xiong Y, Jiang J, Zhang Y, Tian Z and Yan H. γ-Aminobutyric acid inhibits the proliferation and increases oxaliplatin sensitivity in human colon cancer cells. Tumour Biol. 2016;37(11):14885-14894.

10. Stoskus M, Vaitkeviciene G, Eidukaite A and Griskevicius L. ETV6/RUNX1 transcript is a target of RNA-binding protein IGF2BP1 in t(12;21)(p13;q22)-positive acute lymphoblastic leukemia. Blood Cells Mol Dis. 2016;57:30-4.

11. Menezes-Souza D, de Oliveira Mendes TA, de Araújo Leão AC, de Souza Gomes M, Fujiwara RT and Bartholomeu DC. Linear B-cell epitope mapping of MAPK3 and MAPK4 from Leishmania braziliensis: implications for the serodiagnosis of human and canine leishmaniasis. Appl Microbiol Biotechnol. 2015;99(3):1323-36.

12. Rousseau J, Klinger S, Rachalski A, Turgeon B, Déléris P, Vigneault E, et al. Targeted inactivation of Mapk4 in mice reveals specific nonredundant functions of Erk3/Erk4 subfamily mitogen-activated protein kinases. Mol Cell Biol. 2010;30(24):5752-63.

13. El-Aarag SA, Mahmoud A, Hashem MH, Abd Elkader H, Hemeida AE and ElHefnawi M. In silico identification of potential key regulatory factors in smoking-induced lung cancer. BMC Med Genomics. 2017;10(1):40.

14. Wang W, Shen T, Dong B, Creighton CJ, Meng Y, Zhou W, et al. MAPK4 overexpression promotes tumor progression via noncanonical activation of AKT/mTOR signaling. J Clin Invest. 2019;29(3):1015-1029.

15. Wang F, Fu X, Wu X, Zhang J, Zhu J, Zou Y, et al. Bone marrow derived M2 macrophages protected against lipopolysaccharide-induced acute lung injury through inhibiting oxidative stress and inflammation by modulating neutrophils and T lymphocytes responses. Int Immunopharmacol. 2018;61:162-168.

16. Soni S, Wilson MR, O'Dea KP, Yoshida M, Katbeh U, Woods SJ, et al. Alveolar macrophage-derived microvesicles mediate acute lung injury. Thorax. 2016;71(11):1020-1029.

17. Zhao J, Chen C, Guo M, Tao Y, Cui P, Zhou Y, et al. MicroRNA-7 deficiency ameliorates the pathologies of acute lung injury through elevating KLF4. Front Immunol. 2016;7:389.

18. Baker KE, Bonvini SJ, Donovan C, Foong RE, Han B, Jha A, et al. Novel drug targets for asthma and COPD: lessons learned from in vitro and in vivo models. Pulm Pharmacol Ther. 2014;29(2):181-98.

19. Wang B, Xiao Y, Yang X, He Y, Jing T, Wang W, et al. Protective effect of dihydromyricetin on LPS-induced acute lung injury. J Leukoc Biol. 2018.

20. Goodman RB, Pugin J, Lee JS and Matthay MA. Cytokine-mediated inflammation in acute lung injury. Cytokine Growth Factor Rev. 2003;14(6):523-35.

21. Chen H, Bai C and Wang X. The value of the lipopolysaccharide-induced acute lung injury model in respiratory medicine. Expert Rev Respir Med. 2010;4(6):773-83.

22. Refai A, Gritli S, Barbouche MR and Essafı M. Mycobacterium tuberculosis virulent factor ESAT-6 drives macrophage differentiation toward the pro-inflammatory M1 phenotype and subsequently switches it to the anti-inflammatory M2 phenotype. Front Cell Infect Microbiol. 2018;8:327.

23. Yeh CH, Yang JJ, Yang ML, Li YC and Kuan YH. Rutin decreases lipopolysaccharide-induced acute lung injury via inhibition of oxidative stress and the MAPK-NF-κB pathway. Free Radic Biol Med. 2014;69:249-57.

24. Shen HH, Yang CY, Kung CW, Chen SY, Wu HM, Cheng PY et al. Raloxifene inhibits adipose tissue inflammation and adipogenesis through Wnt regulation in ovariectomized rats and 3 T3-L1 cells. J Biomed Sci. 2019;26(1):62.

25. Yan J, Li J, Zhang L, Sun Y, Jiang J, Huang Y, et al. Nrf2 protects against acute lung injury and inflammation by modulating TLR4 and Akt signaling. Free Radic Biol Med. 2018;121:78-85.

26. Aberg E, Torgersen KM, Johansen B, Keyse SM, Perander M and Seternes OM. Docking of PRAK/MK5 to the atypical MAPKs ERK3 and ERK4 defines a novel MAPK interaction motif. J Biol Chem. 2009;284(29):19392-401.

27. Radpour R, Kohler C, Haghighi MM, Fan AX, Holzgreve W and Zhong XY. Methylation profiles of 22 candidate genes in breast cancer using high-throughput MALDI-TOF mass array. Oncogene. 2009;28(33):2969-78.

28. Maurano MT, Wang H, John S, Shafer A, Canfield T, Lee K, et al. Role of DNA methylation in modulating transcription factor occupancy. Cell Rep. 2015;12(7):1184-95.

29. Basith S, Manavalan B, Shin TH and Lee G. SDM6A: A Web-based integrative machine-learning framework for predicting 6mA sites in the rice genome. Mol Ther Nucleic Acids. 2019;18:131-141.

30. Zhang Y, Lu Y, Ji H and Li Y. Anti-inflammatory, anti-oxidative stress and novel therapeutic targets for cholestatic liver injury. Biosci Trends. 2019;13(1):23-31.

31. Escoter-Torres L, Caratti G, Mechtidou A, Tuckermann J, Uhlenhaut NH and Vettorazzi S. Fighting the fire: mechanisms of inflammatory gene regulation by the Glucocorticoid Receptor. Front Immunol. 2019;10:1859.

32. Cartwright T, Perkins ND and L Wilson C. NFKB1: a suppressor of inflammation, ageing and cancer. FEBS J. 2016;283(10):1812-22.

33. Qian F, Deng J, Lee YG, Zhu J, Karpurapu M, Chung S, et al. The transcription factor PU.1 promotes alternative macrophage polarization and asthmatic airway inflammation. J Mol Cell Biol. 2015;7(6):557-67.

34. Yamaguchi R, Sakamoto A, Yamaguchi R, Haraguchi M, Narahara S, Sugiuchi H, et al. Transcription factor specificity protein 1 modulates TGFβ1/Smad signaling to negatively regulate SIGIRR expression by human M1 macrophages stimulated with substance P. Cytokine. 2018;108:24-36.

35. Cargnello M and Roux PP. Activation and function of the MAPKs and their substrates, the MAPK-activated protein kinases. Microbiol Mol Biol Rev. 2011;75(1):50-83.

36. Arthur JS and Ley SC. Mitogen-activated protein kinases in innate immunity. Nat Rev Immunol. 2013;13(9):679-92.

37. Wilhelmsen K, Xu F, Farrar K, Tran A, Khakpour S, Sundar S, et al. Extracellular signal-regulated kinase 5 promotes acute cellular and systemic inflammation. Sci Signal. 2015;8(391):ra86.

38. Carnesecchi S, Deffert C, Pagano A, Garrido-Urbani S, Métrailler-Ruchonnet I, Schäppi M, et al. NADPH oxidase-1 plays a crucial role in hyperoxia-induced acute lung injury in mice. Am J Respir Crit Care Med. 2009;180(10):972-81.

39. Schnyder-Candrian S, Quesniaux VF, Di Padova F, Maillet I, Noulin N, Couillin I, et al. Dual effects of p38 MAPK on TNF-dependent bronchoconstriction and TNF-independent neutrophil recruitment in lipopolysaccharide-induced acute respiratory distress syndrome. J Immunol. 2005;175(1):262-9.

40. Chen W, Zhang X, Fan J, Zai W, Luan J, Li Y, et al. Tethering Interleukin-22 to apolipoprotein A-I ameliorates mice from acetaminophen-induced liver injury. Theranostics. 2017;7(17):4135-4148.

41. Perander M, Al-Mahdi R, Jensen TC, Nunn JA, Kildalsen H, Johansen B, et al. Regulation of atypical MAP kinases ERK3 and ERK4 by the phosphatase DUSP2. Sci Rep. 2017;7:43471.

42. Yin Y, Morgunova E, Jolma A, Kaasinen E, Sahu B, Khund-Sayeed S, et al. Impact of cytosine methylation on DNA binding specificities of human transcription factors. Science. 2017;356(6337). pii: eaaj2239.

43. Wang T, Li J, Ding K, Zhang L, Che Q, Sun X, et al. The CpG dinucleotide adjacent to a κB site affects NF-κB function through its methylation. Int J Mol Sci. 2017;18(3). pii: E528.

44. Wang HM, Ma JD, Jin L, Liu YH, Che TD, Li MZ, et al. Developmental methylation pattern regulates porcine GPR120 expression. Genet Mol Res. 2016;15(1).

45. Convertini P, Todisco S, De Santis F, Pappalardo I, Iacobazzi D, Castiglione Morelli MA, et al. Transcriptional regulation factors of the human mitochondrial aspartate/glutamate carrier gene, Isoform 2 (SLC25A13): USF1 as basal factor and FOXA2 as sctivator in liver cells. Int J Mol Sci. 2019;20(8).

46. Adamzik M, Frey UH, Rieman K, Sixt S, Beiderlinden M, Siffert W, et al. Insertion/deletion polymorphism in the promoter of NFKB1 influences severity but not mortality of acute respiratory distress syndrome. Intensive Care Med. 2007;33(7):1199-1203.

47. Zhao Y, Zhang M, Xiong RP, Chen XY, Li P, Ning YL, et al. Somatostatin reduces the acute lung injury of mice via increasing the affinity of glucocorticoid receptor. Cell Physiol Biochem. 2016;38(4):1354-64.

48. Chen C, Yue D, Lei L, Wang H, Lu J, Zhou Y, et al. Promoter-operating targeted expression of gene therapy in cancer: Current stage and prospect. Mol Ther Nucleic Acids. 2018;11:508-514.

49. Lee TJ, Yoo JY, Shu D, Li H, Zhang J, Yu JG, et al. RNA nanoparticle-based targeted therapy for glioblastoma through inhibition of oncogenic miR-21. Mol Ther. 2017;25(7):1544-1555.

50. Muralidharan R, Babu A, Amreddy N, Srivastava A, Chen A, Zhao YD, et al. Tumor-targeted nanoparticle delivery of HuR siRNA inhibits lung tumor growth in vitro and in vivo by disrupting the oncogenic activity of the RNA-binding protein HuR. Mol Cancer Ther. 2017;16(8):1470-1486.

51. Lei L, Chen C, Zhao J, Wang H, Guo M, Zhou Y, et al. Targeted expression of miR-7 operated by TTF-1 promoter inhibited the growth of human lung cancer through the NDUFA4 pathway. Mol Ther Nucleic Acids. 2017;6:183-197.

52. Tao YJ, Li YJ, Zheng W, Zhao JJ, Guo MM, Zhou Y, et al. Antisense oligonucleotides against microRNA-21 reduced the proliferation and migration of human colon carcinoma cells. Cancer Cell Int. 2015;15:77.

53. Wei L, Li J, Han Z, Chen Z and Zhang Q. Silencing of lncRNA MALAT1 prevents inflammatory injury after lung transplant ischemia-reperfusion by downregulation of IL-8 via p300. Mol Ther Nucleic Acids. 2019;18:285-297.

# Figures

Figure 1

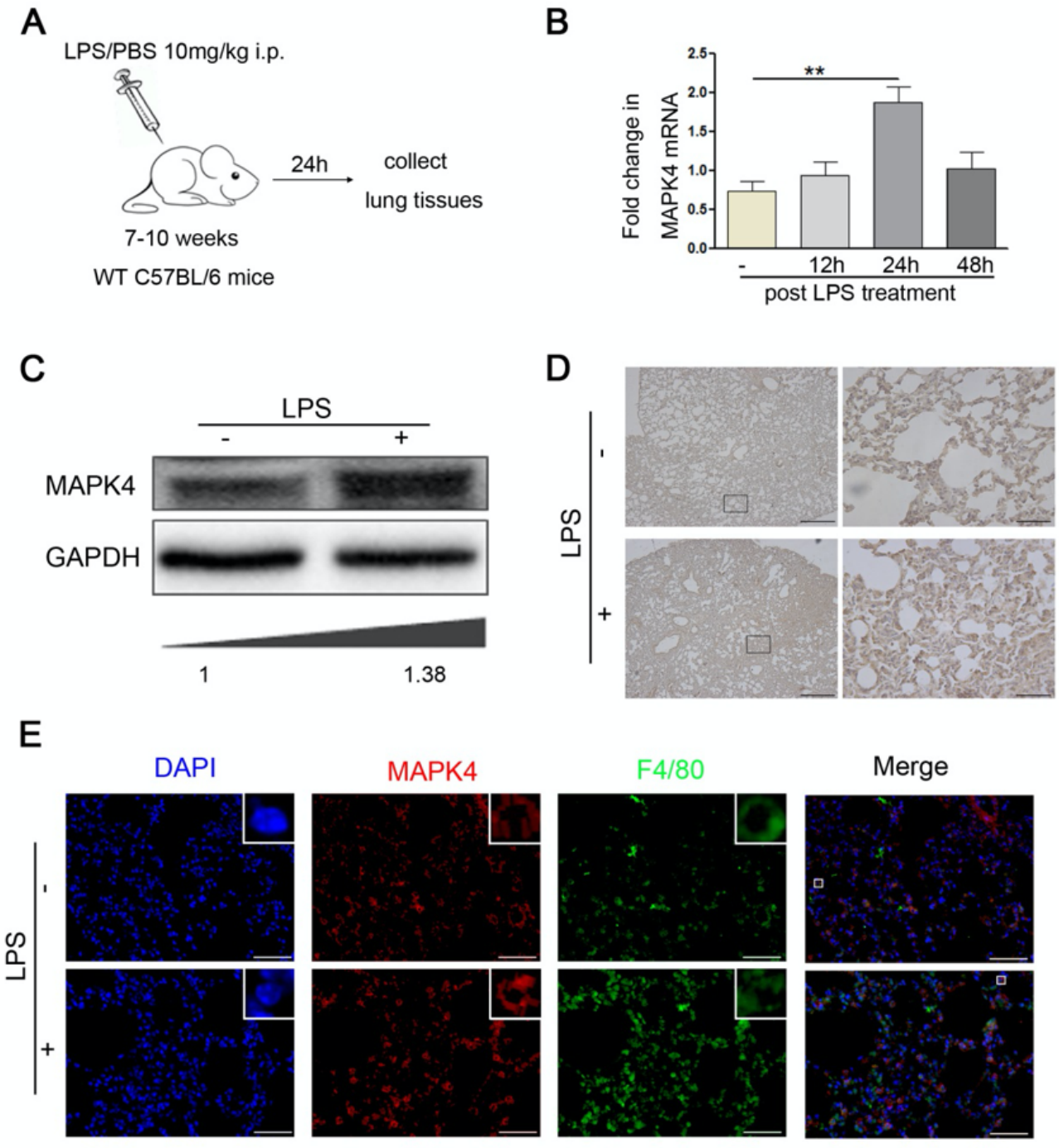


**Figure 1**

MAPK4 is up-regulated in the lung tissues of murine ALI. (A) Wild-type C57BL/6 mice (n=5) were administered with i.p. 10mg/kg LPS or PBS, respectively. After 24h, lung tissues were obtained. (B) The mRNA levels of MAPK4 in lung tissues were detected by Real-time PCR assay. (C-E) The protein levels of MAPK4 in lung tissues were analyzed by western blot, immunohistochemistry and immunofluorescence, respectively. Date are representative at least three independent experiments. **p<0.01.

Figure 2

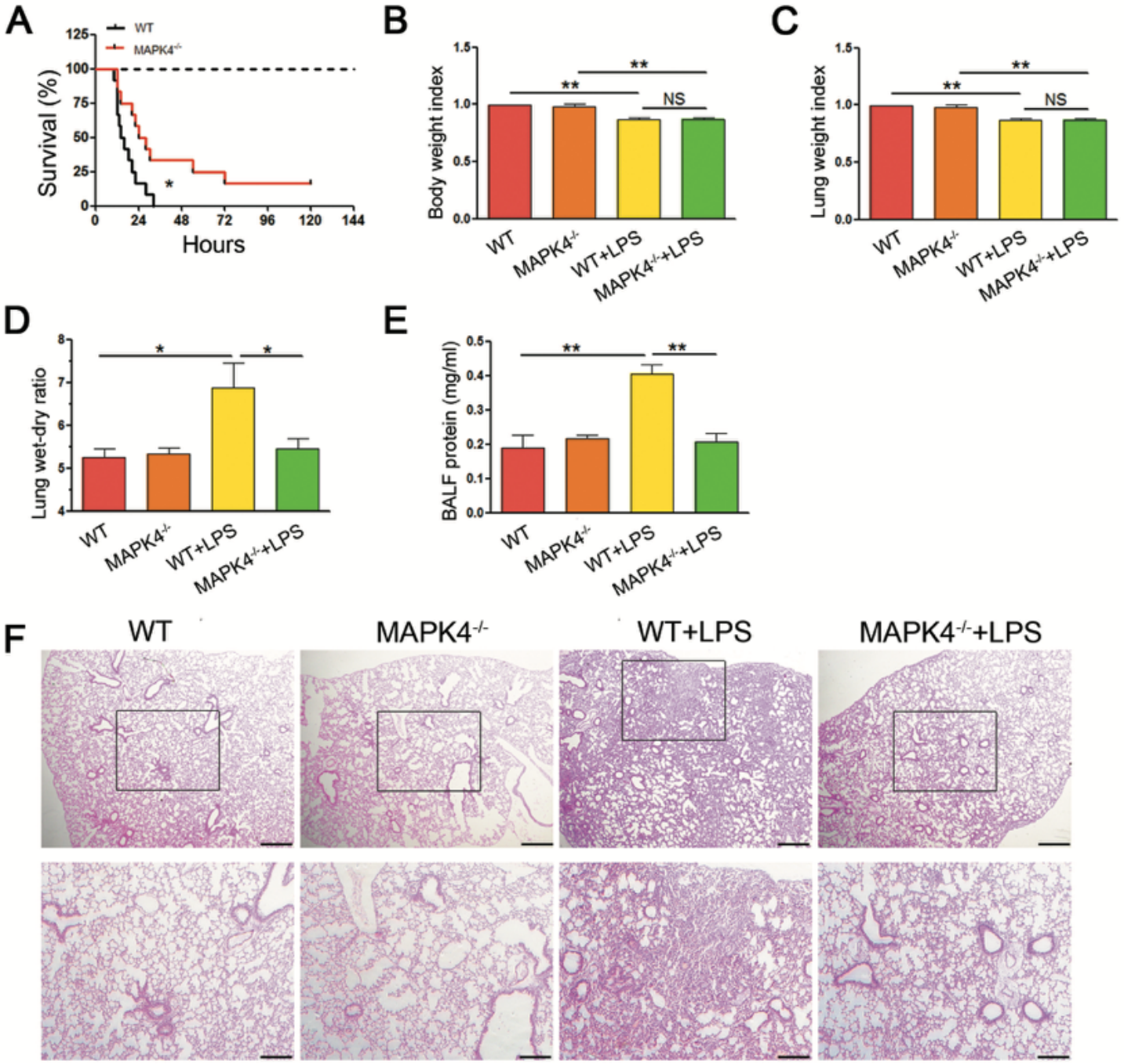


## Figure 2

MAPK4 deficiency ameliorates the pathology of ALI. (A) Wild-type and MAPK4-/- mice were administered with i.p. 15mg/kg LPS, respectively. The survival curve of WT and MAPK4-/- mice (n=12) were recorded. Then, wild-type and MAPK4-/- mice were administered with i.p. 10mg/kg LPS, respectively. (B) The weight index (C) lung weight index (lung weight/weight) , (D) lung wet-dry ratio, (E) protein concentration in BAL fluid were observed after 24h of LPS treatment, respectively. (F) The pathology of lung tissues were

analyzed after 24h with LPS treatment, respectively. Date are representative at least three independent experiments. *p<0.05, **p<0.01.

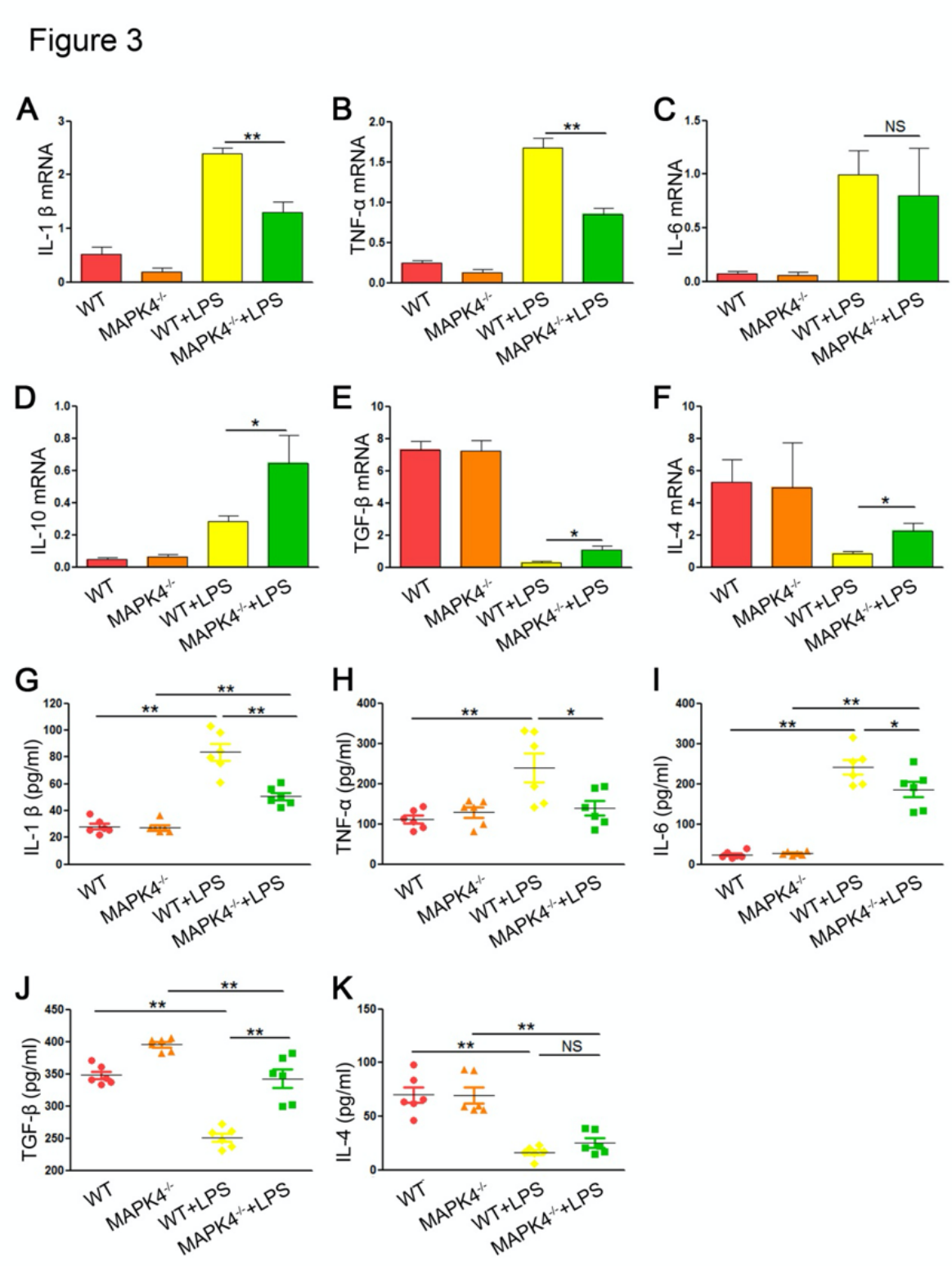


## Figure 3

MAPK4 deficiency alters the production of related cytokines in ALI. Wild-type and MAPK4-/- mice (n=6) were administered with i.p. 10mg/kg LPS, respectively. (A-F) The relative expressions of IL-1β, IL-6, TNF-α, IL-10 and IL-4, as well as TGF-β, in lung tissues were analyzed by Real-time PCR assay and calculated. (G-

K) The protein levels of IL-1β, IL-6, TNF-α, IL-4, TGF-β in BAL fluid were detected by ELISA assay and calculated. Date are representative at least three independent experiments. *p<0.05, **p<0.01.

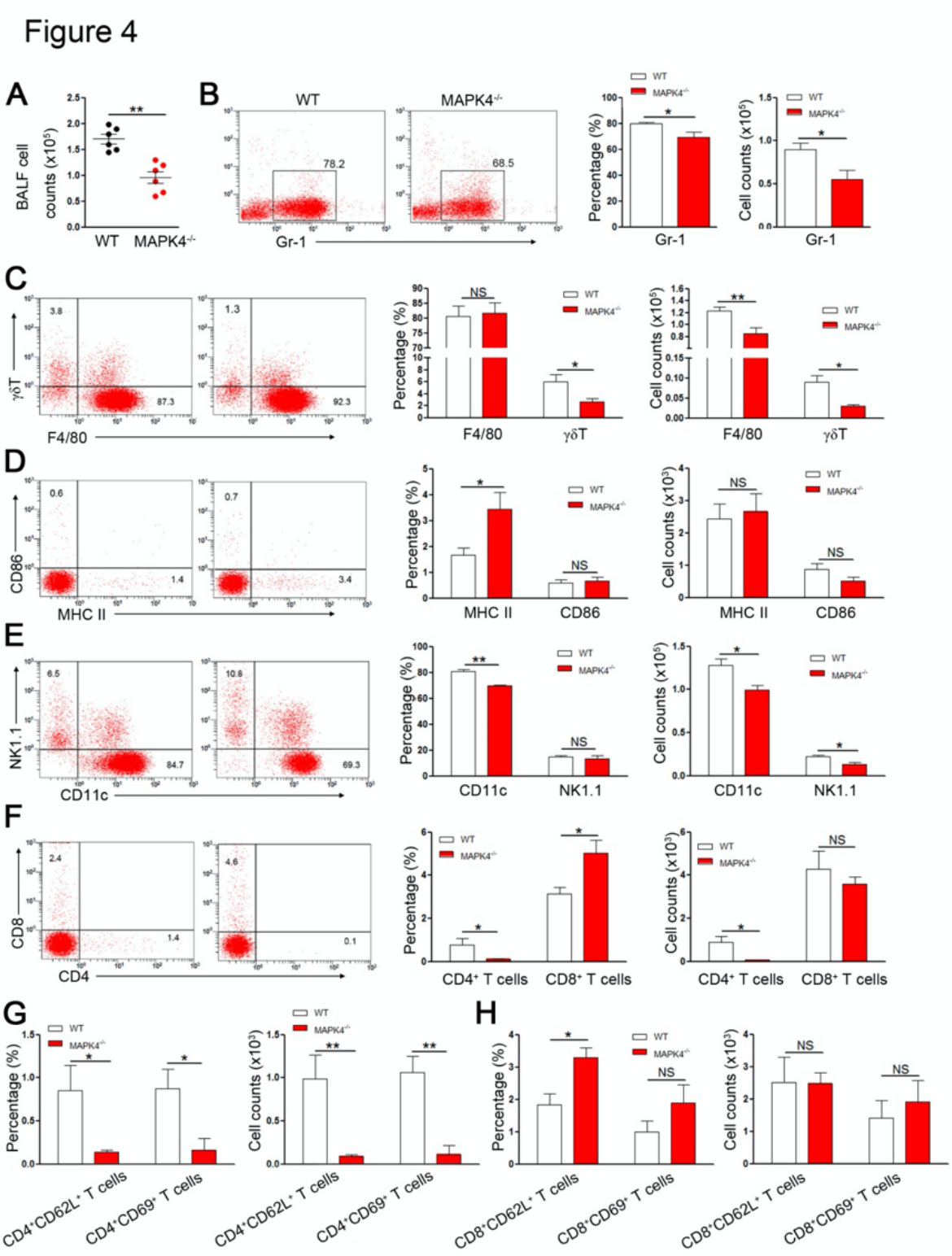


## Figure 4

MAPK4 deficiency affects the immune cells composition in BALF of ALI. Wild-type and MAPK4-/- mice (n=6) were administered with i.p. 10mg/kg LPS, 24h, respectively. Then, the bronchoalveolar cells were collected. (A) Bronchoalveolar total cell counts were counted. (B) The proportions of Gr-1+ neutrophils

were analyzed by FCM and the absolute numbers of these cells were calculated, respectively. (C) The proportions of F4/80+ Mφ and γδ+ T cells were analyzed by FCM and the absolute numbers of these cells were calculated, respectively. (D) The proportions of CD86 and MHC II on F4/80+ Mφ were analyzed by FCM and the absolute numbers of these cells were calculated, respectively. (E) The proportions of CD11c+ dendritic cells and NK1.1+ T cells were analyzed by FCM and the absolute numbers of these cells were calculated, respectively. (F) The proportions of CD4+ T and CD8+ T cells were analyzed by FCM and the absolute numbers of these cells were calculated, respectively. (G) The proportions of CD62L and CD69 on CD4+ T cells or (H) CD8+ T cells were analyzed by FCM and the absolute numbers of these cells were calculated, respectively. Date are representative at least three independent experiments. *p<0.05, **p<0.01.

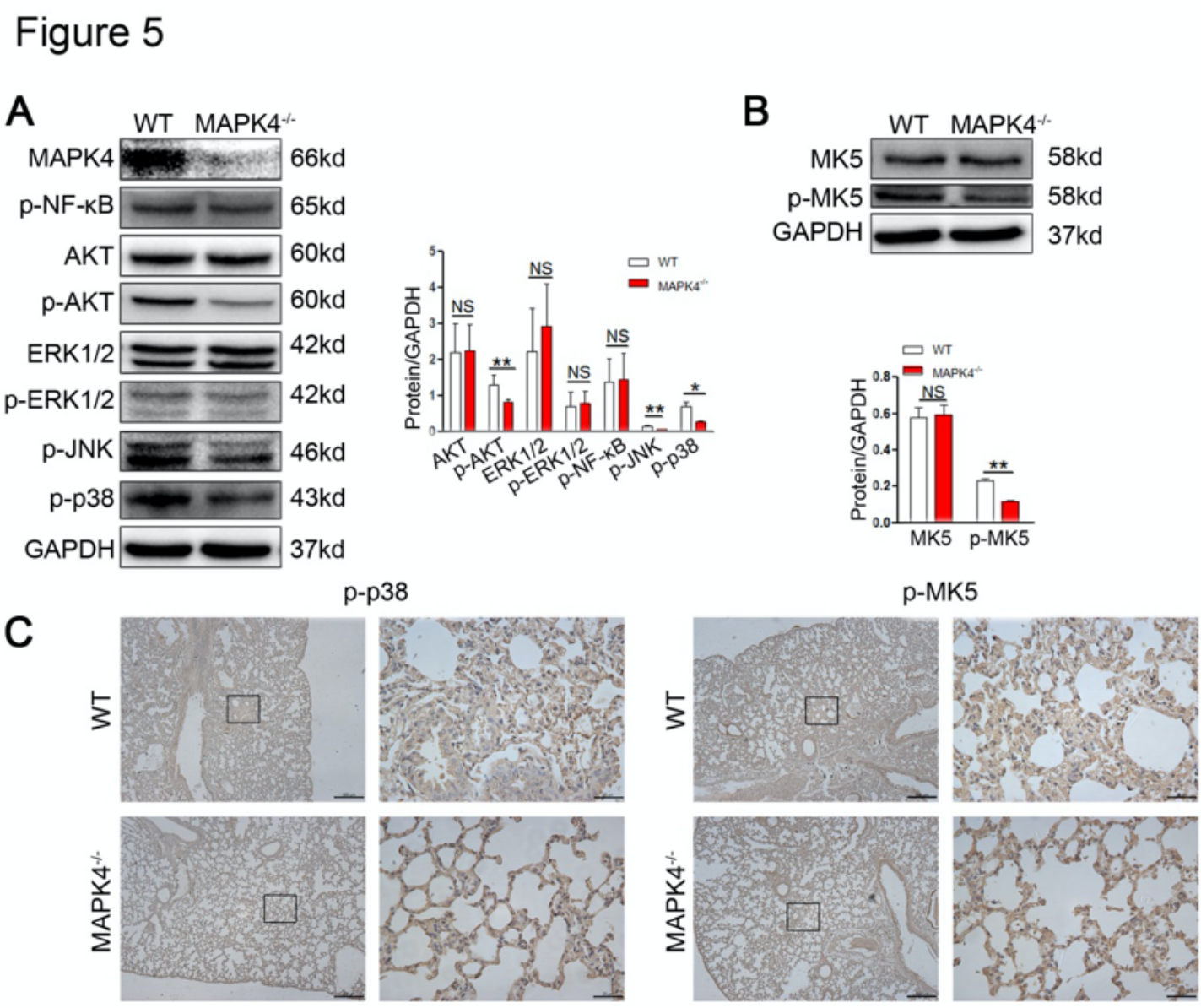


Figure 5

MAPK4 deficiency alters the transduction of related signaling pathways in ALI. Wild-type and MAPK4-/- mice (n=6) were administered with i.p. 10mg/kg LPS, respectively. After 24h, lung tissues were obtained. (A-B) The expressions of MAPK4, ERK, p-ERK, AKT, p-AKT, p-NF-κB, p-p38 MAPK, p-JNK, MK5, p-MK5 were detected by western blot. (C) The expressions of p-p38 MAPK and p-MK5 were detected by immunohistochemistry. Date are representative at least three independent experiments. *p<0.05, **p<0.01.

Figure 6

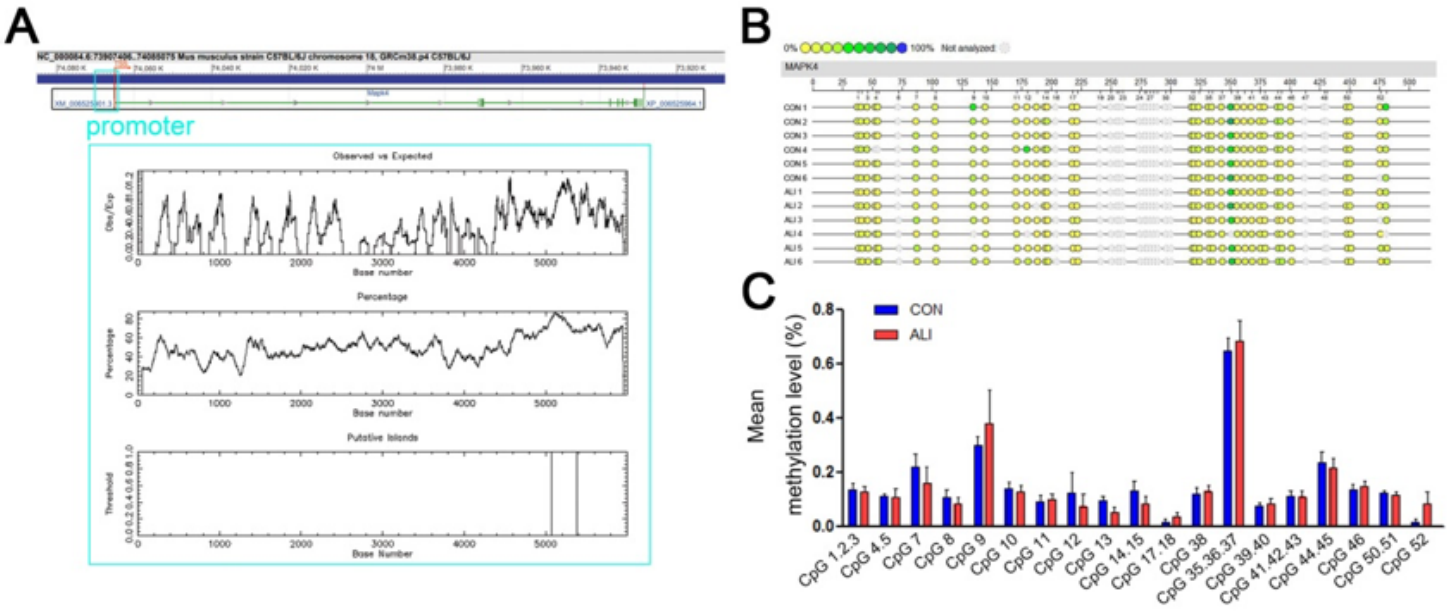


**Figure 6**

CpG methylation levels of MAPK4 promoter in WT and ALI mice. Wild-type mice were administered with i.p. 10mg/kg LPS or PBS, respectively. After 24h, lung tissues were obtained and DNA was extracted. (A) The CpG island was found in the promoter of MAPK4. (B-C) Methylation levels of CpG sites in MAPK4 promoter were observed in 6 paired WT and ALI lungs tissues. Date are representative at least three independent experiments.

Figure 7

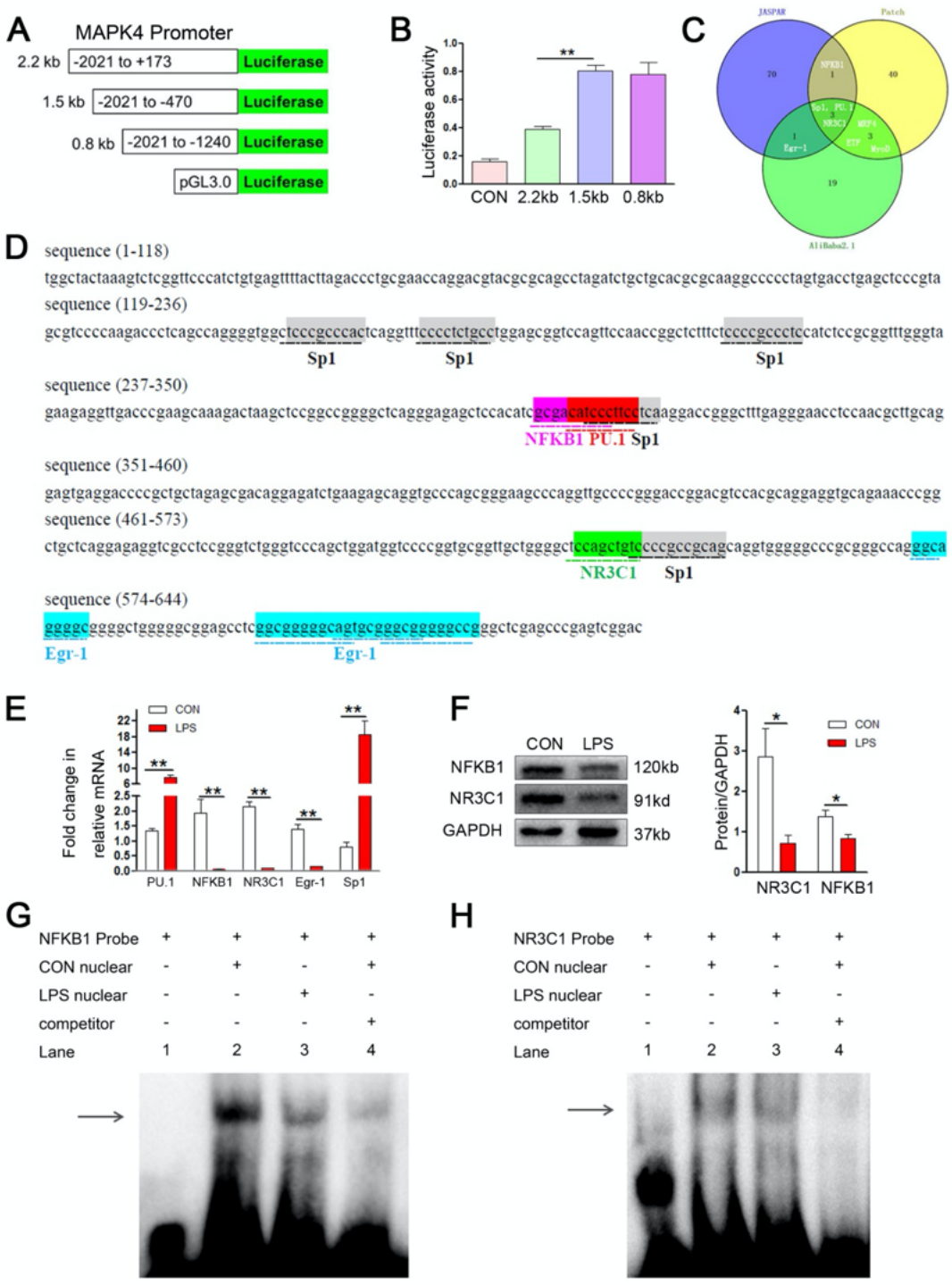


## Figure 7

NFKB1 and NR3C1 are the core transcription factors of MAPK4 in ALI. (A) Series truncated versions of MAPK4 promoter (-2021bp to +173bp) were synthesized and cloned into the luciferase reporter vector pGL3.0 basic. (B) The truncated versions of MAPK4 promoter were transfected into RAW264.7 cells and the relative luciferase activity were measured. (C-D) The candidate transcription factors, including Sp1, MyoD, Egr-1, NFKB1, ETF, PU.1, NR3C1 and MRF4 were screened by TRANSFAC and JASPAP database.

(E) The mRNA levels of relative candidate transcription factors, including PU.1, NFKB1, NR3C1, Egr-1 and Sp1 were detected by Real-time PCR assay. (F) The protein levels of NFKB1 and NR3C1 were analyzed by western blot. (G-H) EMSA assay shows DNA-protein interaction of NFKB1 and NR3C1 transcription factors to the MAPK4 promoter in vitro. Date are representative at least three independent experiments. *p<0.05, **p<0.01.

Figure 8

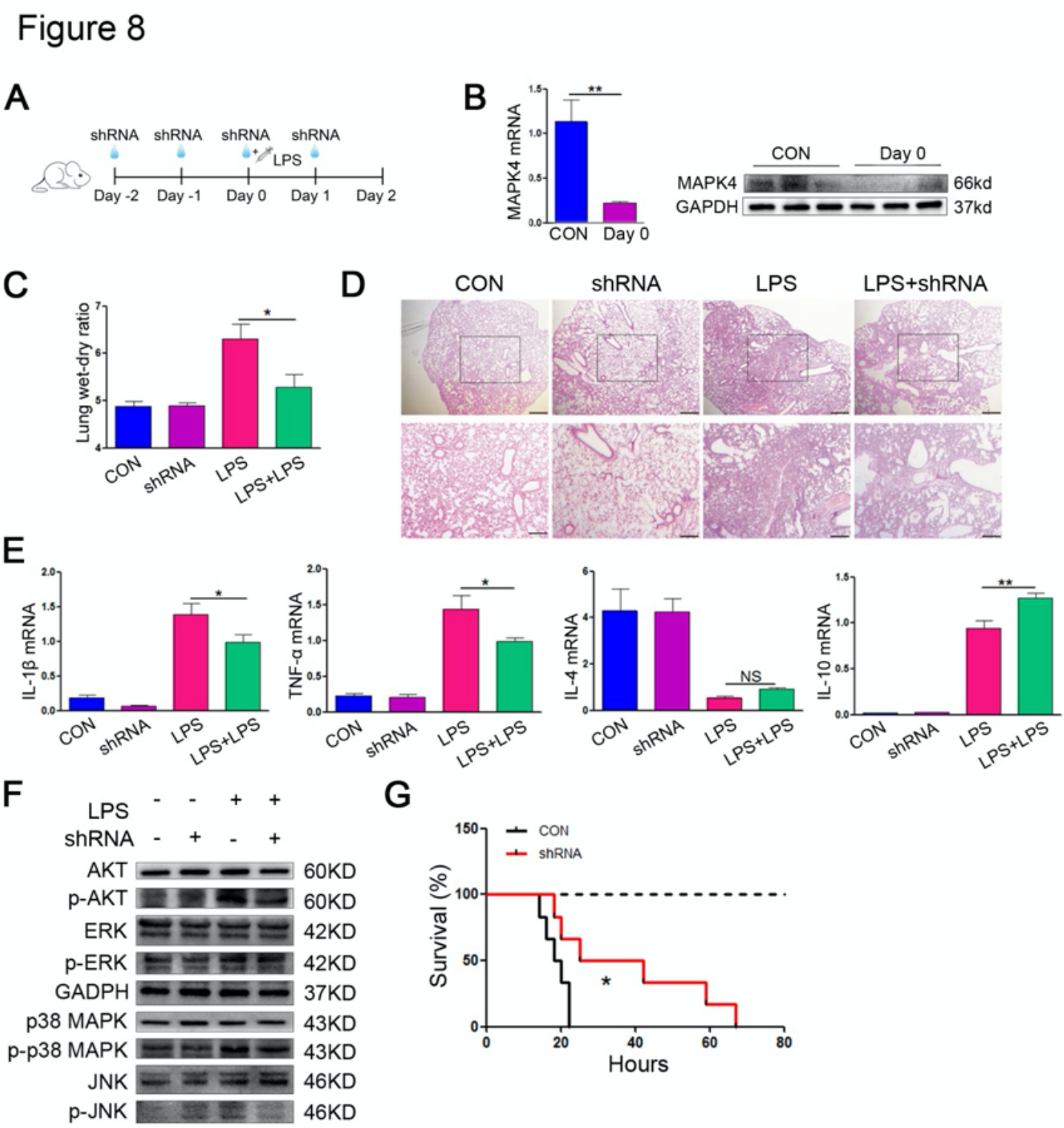


Figure 8

MAPK4-shRNA treatment protects mice against LPS-induced ALI. (A) Schematic diagram showing WT mice were treated with i.t. 10ug MAPK4-shRNA or control vector, then mice were administered with i.p. 10mg/kg LPS in day 0, respectively. (B) Lung tissues were obtained in day 0 and the relative expression of MAPK4 was detected by Real-time PCR assay and western blot. (C) Lung tissues were obtained in day 2 and the lung wet-dry ratio were detected. (D) The pathology of lung tissues were analyzed by HE staining in day 2. (E) The mRNA levels of IL-1β, TNF-α, IL-4 and IL-10 were detected by Real-time PCR assay in day 2. (F) The expressions of ERK, p-ERK, AKT, p-AKT, p38 MAPK, p-p38 MAPK, JNK and p-JNK were detected by western blot in day 2. (G) The survival ratio of CON and MAPK4-shRNA mice (n=6) administered with i.p. 15 mg/kg LPS were recorded, respectively. Date are representative at least three independent experiments. *p<0.05, **p<0.01.

## Supplementary Files

This is a list of supplementary files associated with this preprint. Click to download.

- Supplementaryinformation.docx